**A New Method to Invert for Interseismic Deep Slip Along Closely Spaced Faults using Surface Velocities and Subsurface Stressing-Rate Tensors**

H. Elston[1*], M. Cooke[1], J. Loveless[2], and S. Marshall[3]

[1] *Department of Earth, Geography and Climate Sciences, University of Massachusetts, Amherst, MA, USA*

[2]*A Department of Geosciences, Smith College, Northampton, MA, USA*

[3] *Department of Geological and Environmental Sciences, Appalachian State University, Boone, NC, USA*

Contents of this file

Introduction

The supporting information includes five figures that show additional details related to assessing the completeness and declustering microseismicity (S1) and inverse model results (S2-5). Figure S2 shows the results of inverting 60 different stressing-rate tensor configurations for the simple, single fault model that has three different locking depths. Figures S3 and S4 show the impact of including the basal crack that is included in the long-term forward model in both the interseismic forward model and the inverse model. Figure S5 shows the misfit for complex fault model inversions that utilize a range of smoothing weights.
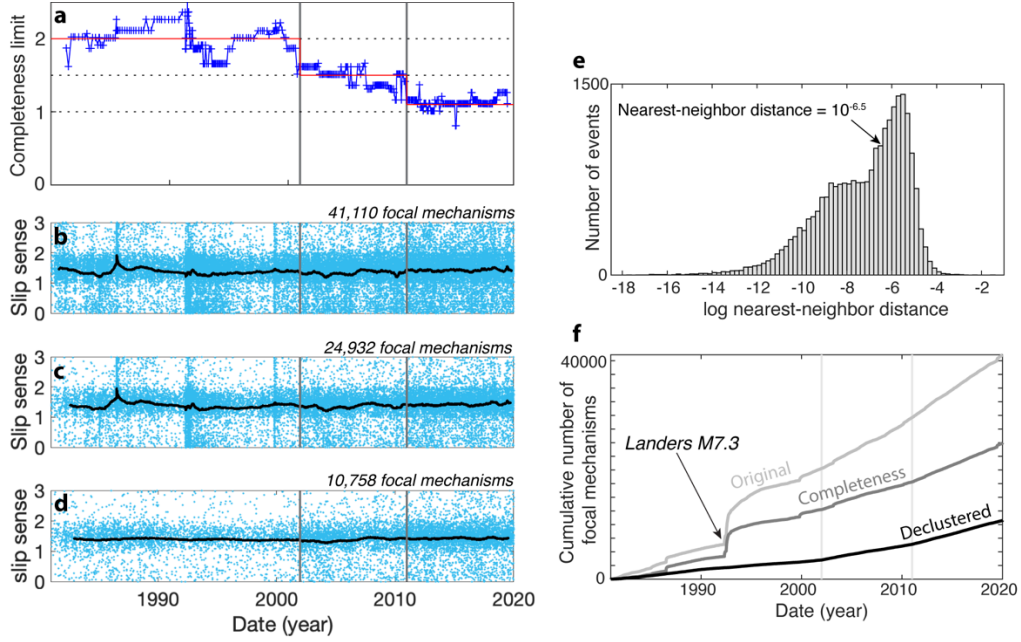
Figure S1. *a) Blue crosses indicate the completeness magnitude calculated for every 1000 events moving forward in increments of 100 events. The vertical grey lines separate the three epochs for which we define a different completeness limit. From 1981 to 2001, the average completeness limit is magnitude 2.0. The limit decreases to magnitude 1.5 in 2002 until 2011 when the limit decreases again to magnitude 1.1. Each point on b-d represent a single event. We calculate the slip sense of each event following (Simpson, 1997). The black line represents the average slip sense for windows of 500 events. A constant average over time suggests that the catalog of events is representative of background seismicity. b) The original catalog from Yang et al. (2012) for the region of interest, which includes 41,110 events. c) The 24,932 events remaining after the completeness assessment. d) The 10,758 events remaining after declustering the catalog. e) Histogram showing the log of the nearest-neighbor distance for the 24,932 focal mechanisms in the catalog following the completeness assessment. We choose a nearest-neighbor distance that results in a catalog that produces a consistent earthquake rate (black line in f). f) The cumulative number of earthquakes with time for three focal mechanism catalogs: 1) original (light gray), 2) after the completeness assessment (medium gray), and 3) after the completeness assessment and declustering to remove aftershocks (black). The slopes of the lines represent the earthquake rate. In catalogs 1 and 2, there are pronounced steps at times following >M5 earthquakes. For example, after the 1992 Landers M7.3 earthquake catalogs 1 and 2 show a large increase in the earthquake rate (slope) for a few months; these steps suggest that the catalogs include a significant number of aftershocks. Alternatively, catalog 3 has a consistent earthquake rate (slope) that only significantly changes when the completeness limit changes (vertical light gray lines), suggesting that catalog 3 captures background seismicity or at the very least, the background rate of seismicity.*
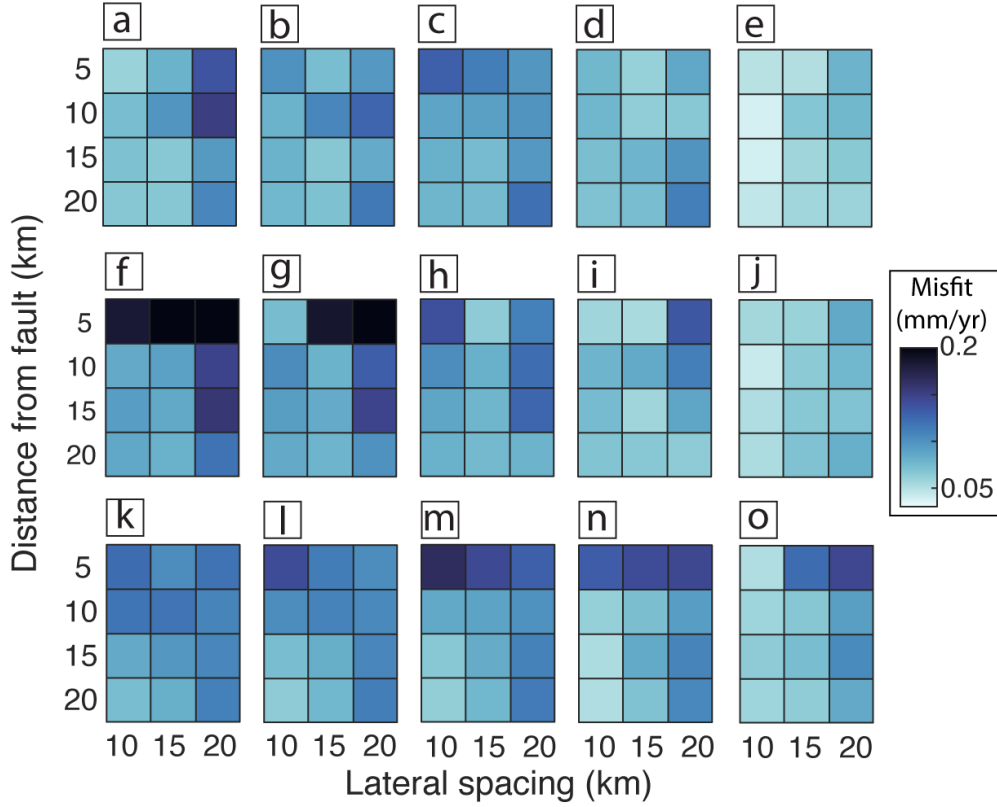
Figure S2. *Misfits calculated for 60 different stressing rate tensor distributions that are generated by forward models with a-e) 10, f-j) 15 or k-o) 20 km locking depths. a-d, f-i, and k-n show misfits for inversions that use on a single row of stressing rate tensor on either side of the fault. Each square indicates the inversion average element misfit in mm/yr. Generally, for stressing-rate tensor distributions at a single depth, as the depth of the tensors increases and the lateral spacing decreases the minimum misfit decreases. Additionally, increasing the distance of the single row of tensors from the fault improves the inversion performance. e, j, and o show misfits for inversions that use two rows of stressing rate tensors on either side of the fault. For all three forward model locking depths, the double row tensor inversions outperform majority of the single row tensor inversions. Double row tensor inversions that have lateral spacing of 10 km and are 5 or 10 km away from the fault produce misfits <0.06 mm/yr for all three forward models. When we apply the inverse approach to the complex fault model and utilize only data where crustal information is available many locations only have stress information at one depth. The results shown here reveal that for single tensor inversions, tensors that are 10 km away from the fault generally outperform single tensor inversions where tensors are 5 km away from the fault. Thus, we use a distance of 10 km away from the fault for the complex fault inversions.*
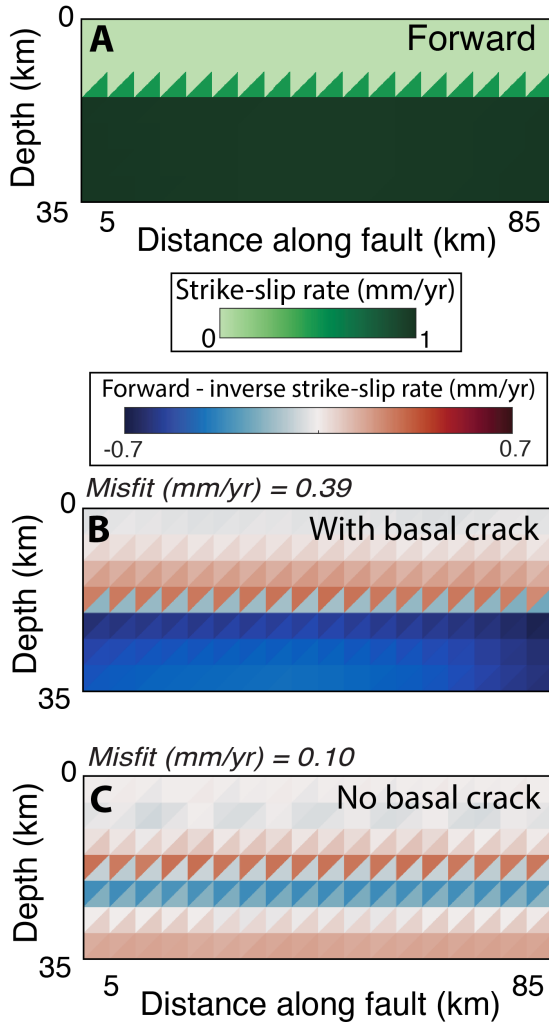
Figure S3. *Slip rate distribution along the fault for the a) interseismic forward model, b) the inversion of surface velocities generated by the forward model that includes the basal crack and c) the inversion of surface velocities generated by the forward model that does not include the basal crack. The inversion of surface velocities that are generated by interseismic forward models that include the horizontal basal crack that simulates deformation below the seismogenic crust (b) does not recover the forward model slip rate distribution as well as models that do not include the basal crack (c). Because the inversion that includes the basal crack performs poorly, we do not include the basal crack in interseismic forward models and inverse models we present in the main text.*
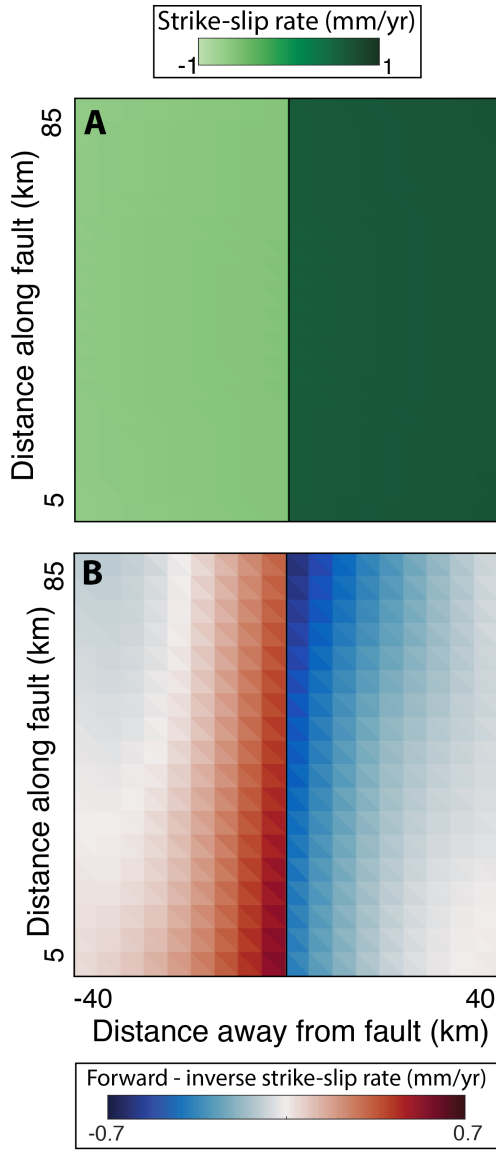
Figure S4. *Slip rate distribution along the horizontal basal crack for the a) interseismic forward model and b) the inversion of forward model generated surface velocities. The black line indicates the fault location. The inversion overestimates slip along the basal crack far from the fault and underestimates slip along the basal crack near the fault.*
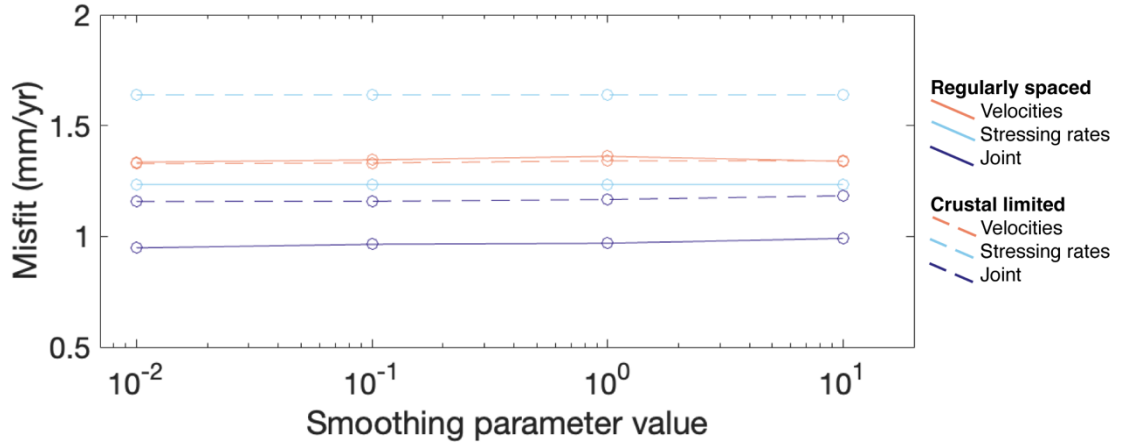
Figure S5. *Area weighted average element misfit for the complex fault model joint and individual inversions that utilize a range of smoothing weights. For the range of smoothing weights we test, the misfit for all inversions varies by < 0.05 mm/yr for each inversion. Solid lines show regularly spaced inversion misfits and dashed lines show crustal limited inversion misfits.*